836 *Biochemistry* **2011,** *50,* 836–842
DOI: 10.1021/bi101648z

BIOCHEMISTRY
including biophysical chemistry & molecular biology
Article

Proton Transfer Facilitated by Ligand Binding. An Energetic Analysis of the Catalytic Mechanism of *Trypanosoma cruzi* Trans-Sialidase[†]

Gustavo Pierdominici-Sottile and Adrian E. Roitberg*

Department of Chemistry and Quantum Theory Project, University of Florida, Gainesville, Florida 32611-8435, United States

Received October 14, 2010; Revised Manuscript Received December 14, 2010

ABSTRACT: Trans-sialidase is a crucial enzyme for the infection of *Trypanosoma cruzi*, the protozoa responsible for Chagas' disease in humans. This enzyme catalyzes the transfer of sialic acids from mammalian host cells to parasitic cell surfaces in order to mask the infection from the host's immune system. It represents a promising target for the development of therapeutics to treat the disease and has been subject of extensive structural studies. Elaborate experiments suggested formation of a long-lived covalent intermediate in the catalytic mechanism and identified a Tyr/Glu pair as an unusual catalytic couple. This requires that the tyrosine hydroxyl proton is transferred to the carboxylate group of glutamate before the nucleophilic attack. Since the solution pK_as of tyrosine and glutamate are very different, this transfer can only be accomplished if the reaction environment selectively stabilizes the product state. We compute the free energy profile for the proton transfer in different environments, and our results indicate that it can take place in the active site of trans-sialidase, but only after substrate binding. By means of the energy decomposition method, we explain the influence that the active site residues exert on the reaction and how the pattern is changed when the substrate is present. This study represents an initial step that can shed light on our understanding of the catalytic mechanism of this reaction.

For enzymatic function, the pK_a values of specific residues are of primary importance. Many reaction mechanisms involving acid/base catalysis require substantially altered pK_as (*1*). These changes in pK_as are possible due to the local environment of the residue. Two well-established cases are mentioned here, but the literature is rife with examples of this behavior. The Glu172 of the xylanase of *Bacillus circulans*, for instance, has a dual role in the mechanism, and its pK_a value changes from ∼7.0 to ∼4.0 during the course of the catalyzed reaction (*2*). In a second example, Glu35 of hen egg white lyzozyme acts as a proton donor, indicating that its pK_a value is higher than the corresponding water solution value (*3*, *4*). It is usually assumed that the energetic cost necessary for a distinct pK_a seen in a protein is prepaid in the folding process mostly in the form of unfavorable dipole−dipole interactions (*5*−*7*).

Sialic acids is the common name for O- and N-substituted derivatives of a nine carbon monosaccharide called neuraminic acid (*8*) . These acids lie on the terminal position of cell surface glycoproteins and glycolipids and are used for recognition by the immune system (*9*, *10*). Sialidases catalyze the removal of sialic acid from various glycoconjugates (*11*). *Trypanosoma cruzi* trans-sialidase (TcTS)[1] is a member of the family of sialidases that transfers sialic acids from donor sialo-glycoconjugates to acceptor glycoconjugates (*12*, *13*) while having a minor straight sialidase activity component. *T. cruzi* is a flagellate protozoan identified as the causative agent of Chagas' disease. This parasite relies in its TcTS enzyme to evade the immune system of the host (*14*−*17*). Due to its importance for the disease, this enzyme is one of the most extensively studied among trans-sialidases (*12*, *13*, *18*−*21*).

In the initial step of the mechanism of TcTS, the sialic acid is scavenged from the donor glycoconjugate with nucleophilic participation of the enzyme (*22*). Whether this nucleophilic participation ends up collapsing into a covalent intermediate or remains as an oxocarbenium ion intermediate has been long discussed for enzymes of similar families, even for the very well studied lysozyme (*3*, *23*, *24*). Kinetic isotope effect studies revealed strong nucleophilic participation and little charge development in the transition state of TcTS, and these results together with the fact that TcTS retains the stereochemistry around the reaction center pointed toward subsequent covalent intermediate formation. Additionally, quenching the catalytic reaction of a radioisotope-labeled ligand indicated that the mechanism involved a covalent bond formation between the ligand and the enzyme (*18*). A separate effort later achieved trapping and identification of the covalent intermediate of TcTS using 2-deoxy-2,3-difluorosialic acid as an activated ligand (*19*, *20*). These activated fluorinated ligands also facilitated identification of Tyr342/Glu230 as an unusual nucleophile couple. Particularly, the hydroxyl oxygen of Tyr342 attacks the anomeric carbon of the sialic acid and forms a covalent intermediate, with a concomitant proton transfer to Glu230 (see Figure 1). This transfer from the hydroxyl group of a tyrosine to a carboxylate group can only be possible if the active site of TcTS selectively stabilizes the product state. In other words, the pK_a values for these residues should be significantly shifted from their water solution values.

In this report we present a theoretical study aimed to explain how this transference can take place in the active site of TcTS, but only after substrate binding. The free energy profiles for this

[†]This work was funded by the National Institutes of Health (NIH 1R01AI073674-01).

*To whom correspondence should be addressed. Phone: (352) 392-6972. Fax: (352) 392-8722. E-mail: roitberg@ufl.edu.

[1]Abbreviations: TcTS, *Trypanosoma cruzi* trans-sialidase; MD, molecular dynamics; MM, molecular mechanics; QM, quantum mechanics; WHAM, weighted histogram analysis method.

 Published on Web 12/16/2010

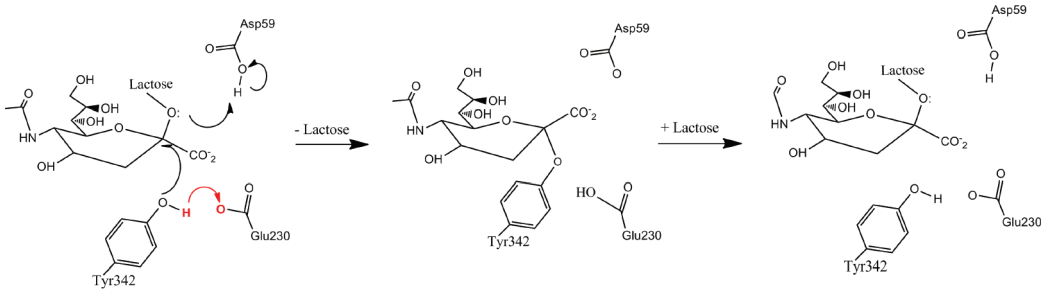

FIGURE 1: The mechanism of sialyl-transfer reaction of TcTS considering a covalent intermediate. The proton transfer from Tyr342 to Glu230 is pointed out in red. This transference needs to take place so as to enable the bond formation between Tyr342 and the sialic acid.

proton transfer reaction in water solution, in the apo (unbound substrate) form of TcTS and in its holo (substrate-bound) form were computed. Our results indicate that ΔG°_{r} (standard free energy change) seen for the holo form is ~10.0 kcal/mol lower than for the apo form, making the transfer plausible in the presence of the substrate and improbable in its absence. This difference between the ΔG°_{r}s could be explained by the distinct electrostatic interaction pattern of the active site residues. Particularly, the biggest changes noticed upon substrate binding belong to the residues of the arginine triad (Arg35, Arg245, and Arg314), and the reason for these changes is mainly due to the different charge distribution (polarization) seen upon the proton transfer in the apo and holo forms of the enzyme.

The rest of the report is organized as follows. The next section explains the methodologies employed in the calculations. Then, we report and discuss the results of such computations. Finally, the conclusions of this work are outlined.

METHODS

General Aspects. Here, we briefly describe the general aspects that were followed for the full QM optimizations, for the free energy calculations, and for the implementation of the energy decomposition method. The details are then explained. QM optimizations were performed using GAUSSIAN09 (*25*) while QM/MM computations presented in this report were achieved by means of the AMBER10 package (*26*), and unless explicitly stated otherwise, the PM3-PDDG level of theory was the one employed to describe the quantum subsystem (*27*). Amber99SB (*28*, *29*) force field was selected to describe the potential energy of the classical region.

The initial configurations of the crystallographic structure of TcTS with sialyllactose (holo form) and without (apo form) were taken from the Protein Data Bank, entries 1MS3 and 1S0I, respectively. In what follows, the residue numbering and the names of the atoms correspond to these crystallographic structures. The systems were protonated considering standard states except for D59. This residue is responsible for the acid/base catalysis, and its aspartic acid form was used. The resulting files were fed into the Leap module of Amber, and the systems were solvated in a TIP3P rectangular parallelepiped water box of 8.0 Å around the solutes, conserving crystallographic water molecules. Molecular dynamics (MD) simulations were performed using periodic boundary conditions with a cutoff distance of 12.0 Å and a time step of 1.0 fs. The particle mesh Ewald method was used to calculate the long-range Coulomb Forces (*30*). The initial structures were minimized at constant volume, and in a second stage, the system was heated from 0 K to a target temperature of 300 K during 55.0 ps using the weak-coupling algorithm (*31*) with a τ_{tp} value of 2.8 ps. During this heating, the volume was kept constant. After this, we switched to constant temperature and pressure conditions, using a value of 2.0 ps for both τ_{tp} and τ_{p}, so that the density could relax. Finally, 300 ps of equilibration MD were practiced. The equilibrated structures were used as the initial points for the umbrella sampling analysis.

Umbrella Sampling Calculations. We evaluated the free energy profile for the proton transfer in three different systems. One of them corresponds to a model containing only residues Tyr342 and Glu230 in a water box. To construct this model, we started from the apo form of the enzyme, cut the bonds linking the Cα atoms to the protein backbone, and then filled the free valence of each Cα with hydrogen atoms. During the MD simulations, a 100.0 kcal/(mol Å^2) harmonic restraint on the Cα atom of both residues was applied to their starting positions so as to mimic the distance in the protein environment. Water molecules were modeled by MM while Tyr342 and Glu230 were part of the QM subsystem. The other two systems were the apo and holo forms of TcTS. All residues of the active site that interacts directly with the substrate were included in the QM region. Particularly, for the apo form of the enzyme the QM subsystem was defined considering the residues Tyr342, Glu230, Arg35, Arg245, Arg314, Asp96, and Glu357. For the holo form case, the sialyllactose was also considered as part of this subsystem. The reaction coordinate was defined as the distance between the proton that is transferred and the acceptor oxygen, $z \equiv$ R(H(Tyr342)−O(Glu230)). The selected oxygen atom of the carboxylate group of Glu230 was the one nearest the H(Tyr342) in the equilibrated configuration. There are of course many possible definitions of the reaction coordinate. However, since we are not interested in the reaction profile, but rather only in the standard free energy of the reaction, the coordinate we chose is computationally efficient to sample conformational space. A set of 18 production MD simulations of 20 ps were performed restraining the reaction coordinate with a harmonic potential with a force constant of 525.0 kcal/mol, starting with a value of 1.96 Å and changing it 0.07 Å up to a value of 0.91 Å. Before each production MD, a 5 ps equilibration phase was carried out. The last structure of each MD in a given umbrella window was used as the initial one to perform the next one for which the value of the reaction coordinate is restraint to the next position. In each MD, the Mulliken charges of the quantum subsystem and the coordinates of the system were saved every 50 fs, while the value of the reaction coordinate was written every 2 fs. The weighted histogram analysis method (WHAM) (*32*) was used to analyze the probability density and to obtain the free energy profiles for the unbiased system along the reaction coordinate. To verify the convergence, we recalculated the free energy profiles using production phases of 30, 60, 100, and 200 ps, and we found that the change in the ΔG°_{r} was < 0.2 kcal/mol for all cases.

Interaction Energy Decomposition. We used the energy decomposition method to understand the differences between the free energy changes for the proton transfer seen upon substrate binding. This method was recently applied by Lin et al. to analyze an internal proton transfer step in Dopa decarboxylase (*33*) and has been extensively applied to enzymes (*34*−*41*). In the present study, we employed it to describe the electrostatic interaction of each residue on the product and reactant state of the apo and holo forms of the enzyme.

The influence of an individual residue on the energy of a particular structure was measured taking into account the difference of energies when a particular residue is present (denoted by i in eq 1) or when it is replaced by Gly ($i - 1$ in eq 1) (*36*, *40*, *41*). When the substrate influence was evaluated, its absence was simulated by treating it as part of the classical subsystem and setting its partial charges equal to zero. Mathematically, the equation to measure the influence of a residue can be written as

$$\Delta E_i = [E_i^{\mathrm{QM}} + E_i^{\mathrm{QM,MM}}] - [E_{i-1}^{\mathrm{QM}} + E_{i-1}^{\mathrm{QM,MM}}] \quad (1)$$

where each term in brackets represents the energy of the QM subsystem influenced by the classical environment. That is

$$E^{\mathrm{QM}} + E^{\mathrm{QM,MM}} = \langle \Psi | H^{\circ}_{\mathrm{QM}} + H_{\mathrm{QM/MM}} | \Psi \rangle \quad (2)$$

where H°_{QM} and $H_{\mathrm{QM/MM}}$ are the Hamiltonians of the QM subsystem and the interactions between the QM and MM regions, respectively. The important quantity to evaluate is the relative interaction of each residue in going from reactants to products.

$$\Delta\Delta E_i = \Delta E_i^{\mathrm{products}} - \Delta E_i^{\mathrm{reactants}} \quad (3)$$

Similar approaches but using distinct level of theories to estimate the gas phase and the interaction energy of the QM subsystem have also been employed and validated (*41*−*47*).

We present the averaged interaction energy of each residue, where 400 snapshots from the umbrella sampling were considered. The cutoff distance was set to 99.0 Å. In this analysis Tyr342 and Glu230 were the residues that constituted the QM subsystem for the apo form of the enzyme, while for the holo form the substrate was also considered part of the QM subsystem. The method was applied for residues whose distance between its center of mass and the center of mass of the reactive center (Tyr342 + Glu230) was <12.0 Å in the crystallographic structure. This includes 75 residues of the active site of TcTS. It is expected that due to the distance toward the reaction center the rest of the system would have basically the same effect for both reactants and products.

RESULTS AND DISCUSSION

The first study was the optimization of the reactant and product configurations of the model system (Tyr342 + Glu230) in vacuum so as to compare the ΔE values for the proton transfer using three distinct levels of theory: MP2/6-31(d,g), PM3, and PM3-PDDG. The *ab initio* result was −2.66 kcal/mol while the PM3 and PM3-PDDG results were −7.21 and −3.09 kcal/mol, respectively. These values show that for this model, although PM3 results are different from the MP2 level of theory, PM3-PDDG can be considered a good method to study the energetics of the system. In a recent review, Acevedo et al. have described the progress that has been made in modeling both solution-phase organic and enzymatic reactions using this level of theory (*48*).

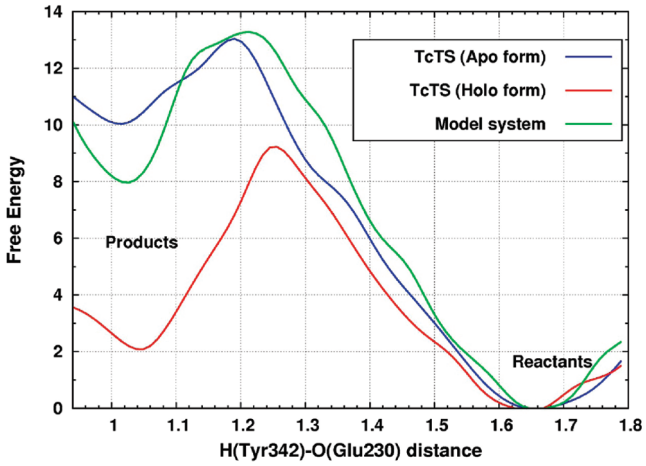

FIGURE 2: Free energy plot for the proton transfer from Tyr342 to Glu230 in the model system (green) and in the apo (blue) and holo (red) form of TcTS. The reaction coordinate was defined as $z \equiv$ R(H(Y342)−O(E230)). Reactant state corresponds to the right side of the graphics. The error values calculated for the data corresponding to the three systems were all below 0.2 kcal/mol.

It should be mentioned that, in what follows, as we are not interested in the kinetics of the process but only in their thermodynamic aspects, we would simply center the discussion on the $\Delta G^{\circ}_{\mathrm{r}}$s and not on the $\Delta G^{\ddagger}_{\mathrm{r}}$s of the reaction.

The standard pK_a value of tyrosine in solution is ~10.1, about 5.8 units higher than the pK_a corresponding to glutamic acid (~4.4). A simple transformation for that ΔpK_a into $\Delta G^{\circ}_{\mathrm{r}}$ provides an estimate of ~8 kcal/mol, showing that the transference of a proton from a tyrosine to a glutamate is unlikely to happen in water. The $\Delta G^{\circ}_{\mathrm{r}}$ we have obtained for the Tyr + Glu model in water was 7.86 kcal/mol, confirming the fact mentioned above and in a somewhat surprising agreement with the simple estimate from the individual pK_as. When the apo form of TcTS is taken into account, the $\Delta G^{\circ}_{\mathrm{r}}$ is 2.3 kcal/mol larger (10.16 kcal/mol), indicating that the enzymatic environment makes this transfer even more unlikely than in water. For the holo form of TcTS, results show that reactants and products are significantly closer ($\Delta G^{\circ}_{\mathrm{r}}$ = 2.11 kcal/mol). Similar results were obtained using the MNDO-PDDG (*27*) level of theory for the quantum subsystem. This decrease in the $\Delta G^{\circ}_{\mathrm{r}}$ value proves that substrate binding substantially increases the probability of a proton transfer from Tyr342 to Glu230. The free energy profiles for the three systems considered are shown in Figure 2. There exist several cases in which the catalytic mechanism requires that the pK_a values of specific residues differ from their water solution values (*2*, *3*, *24*, *49*−*51*). In most cases, these changes are induced by the enzyme environment. However, in the particular case of the apo form of TcTS, the active site residues slightly perturb the pK_a values of Tyr342 and Glu230, making the proton transfer less favorable than in water solution. Interestingly, when sialyllactose is present in the active site, this transfer turns favorable. In this way the enzyme environment keeps Tyr342 protonated when the substrate is absent and, only upon sialyllactose binding, causes a change in the environment that enables Tyr342 to be deprotonated and act as a nucleophile.

To explain the differences in the $\Delta G^{\circ}_{\mathrm{r}}$s between both forms of the enzyme, we made use of the interaction energy decomposition method. In Figure 3, the relative energies (computed according to eq 3) for both forms of TcTS are presented. In the crystallographic configuration, the sialic acid interacts with four residues of the

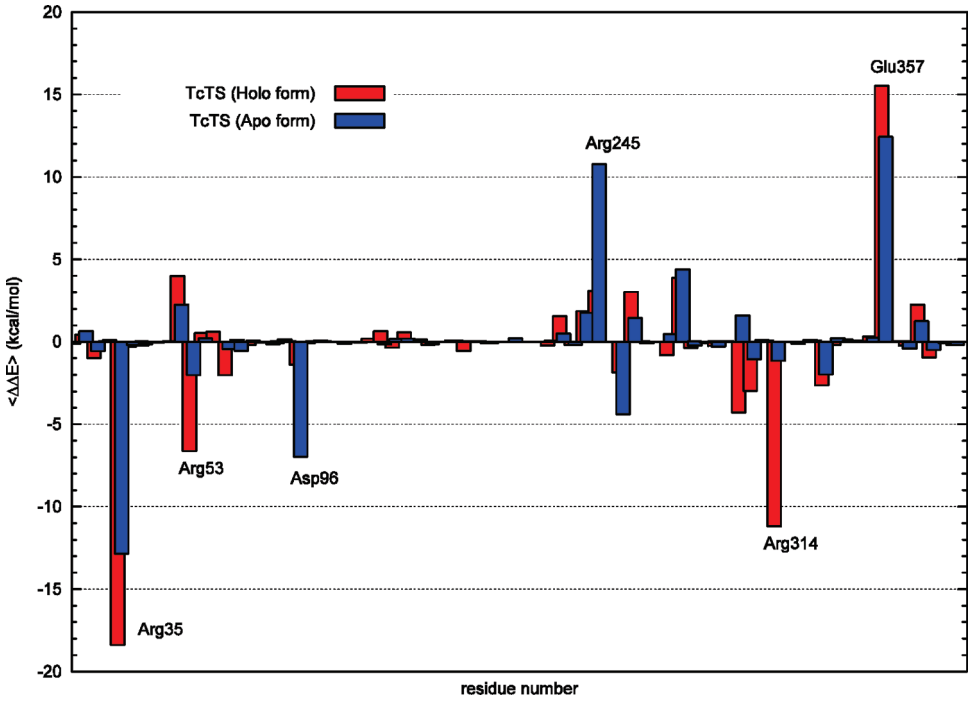

FIGURE 3: Relative stabilization (eq 3) of the active site residues for the transference in the apo and holo form of TcTS. Blue bars represent the values for the apo form of TcTS, while red bars do it for the holo form.

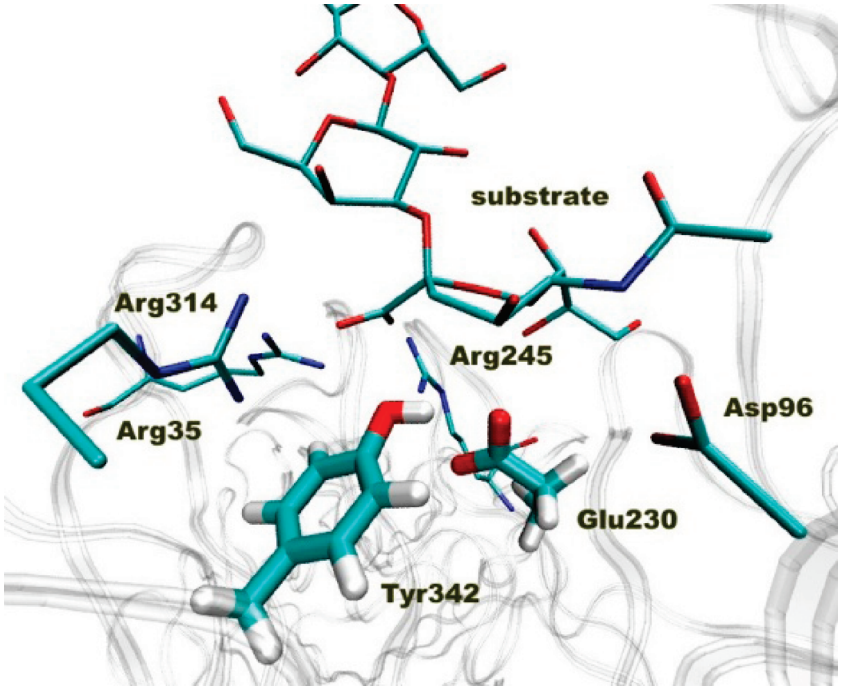

FIGURE 4: Active site of *T. cruzi* trans-sialidase. The proton transfer analyzed is this study takes place between Tyr342 and Glu230. Arg35, Arg245, Arg314, and the substrate (sialyllactose) are also shown. For these residues hydrogen atoms are not shown.

active site: Arg35, Arg245, Arg314, and Asp96. The arginine triad interacts with the carboxylate group of the sialic acid while Asp96 is H-bonded with N12 of the sialic acid (see Figure 4). Besides its interaction with the substrate, Arg245 forms a hydrogen bond with the nonacceptor oxygen atom of the carboxylate group of Glu230. The outcome for the energy decomposition analysis indicates that, for the apo form, Arg35 and Asp96 are the two residues that most stabilize the reaction while Arg245 and Glu357 also have a large effect but destabilizing the transfer. The reason for their effects can be explained in terms of their positioning. Arg35 and Glu357 are close to Tyr342. After transferring the proton, the larger electron density of the tyrosinate is stabilized by Arg35 and destabilized by Glu357. An analogue situation holds true for Asp96 and Arg245, which are close to Glu230. When the global differential interaction is calculated, adding up the contribution of each the 75 residues, it turns out that the enzyme environment destabilizes the transference in 3.22 kcal/mol.

When the holo form is studied, a change in the stabilization pattern is seen, mainly for the arginine triad (see Figure 3 and

Table 1: Values of the Relative Stabilization (eq 3) of the Most Influence Residues of the Active Site Residues for the Transference in the Apo and Holo Form of TcTS[a]

residue	apo TcTS	holo TcTS	difference (holo − apo)
Arg35	−12.84 ± 0.32	−18.39 ± 0.36	−5.55 ± 0.68
Arg53	−2.03 ± 0.21	−6.64 ± 0.25	−4.61 ± 0.46
Asp96	−6.96 ± 0.35	−1.38 ± 0.30	5.58 ± 0.65
Arg245	10.76 ± 0.41	3.05 ± 0.29	−7.71 ± 0.70
Arg314	−1.15 ± 0.19	−11.20 ± 0.27	−10.05 ± 0.46
Glu357	12.43 ± 0.39	15.51 ± 0.43	3.08 ± 0.82
substrate		12.16 ± 0.42	12.16 ± 0.42
rest of the residues	3.01 ± 0.16	−0.29 ± 0.18	−3.30 ± 0.34
total effect for all residues	3.22 ± 0.29	−7.18 ± 0.38	−10.40 ± 0.67

[a]Results are in kcal/mol. The addition for the total effect is done considering the 75 residues analyzed.

Table 2: Average Values and Standard Deviations of the Mulliken Charges for the Atoms of the Carboxylate Group of Glu230 and for the COH Group of Tyr342[a]

	apo form of TcTS		holo form of TcTS	
atom	charge R	charge P	charge R	charge P
C(Glu230)	0.367 ± 0.002	0.383 ± 0.005	0.345 ± 0.003	0.393 ± 0.002
O(Glu230)	−0.710 ± 0.004	−0.571 ± 0.006	−0.721 ± 0.003	−0.615 ± 0.006
acep O(Glu230)	−0.763 ± 0.005	−0.436 ± 0.011	−0.685 ± 0.004	−0.260 ± 0.007
C(Tyr342)	−0.072 ± 0.002	0.095 ± 0.005	−0.084 ± 0.005	0.081 ± 0.003
O(Tyr342)	−0.399 ± 0.005	−0.772 ± 0.004	−0.411 ± 0.004	−0.814 ± 0.005
H(Tyr342)	0.275 ± 0.002	0.291 ± 0.003	0.291 ± 0.003	0.244 ± 0.004

[a]Both reactant and product configurations of the apo and holo form of TcTS are considered.

Table 1). For instance, Arg314 and Arg35, which have a product stabilizing effect of 1.15 and 12.84 kcal/mol for the apo form, in the presence of sialyllactose their product stabilizing effect increases up to 11.20 and 18.39 kcal/mol, respectively. Regarding Arg245, its effect is 10.76 kcal/mol product destabilizing in the apo form, and although it keeps destabilizing the product state in the holo form, it does it in only 3.05 kcal/mol. These changes seen in the pattern of the arginine triad are mainly responsible for the enhancement of the transference observed upon substrate binding. The opposite effect observed for the arginine triad is seen for Asp96, which stabilizes the transference ~5.5 kcal/mol more in the apo than in the holo form. Moreover, the sialyllactose itself has a big destabilizing effect of 12.16 kcal/mol due to the unfavorable interaction, in the product state, between its carboxylate group and the tyrosinate. However, these two effects do not counteract the changes observed for the arginines mentioned above. In fact, the total effect of the environment for the holo form case is to stabilize the product state by 7.18 kcal/mol, being 10.40 kcal/mol lower than the one corresponding to the apo form. This change is responsible for the distinct $\Delta G°_r$s observed in the free energy profiles. Finally, from Table 1 it can also be noticed that the change in the stabilization pattern if we exclude the arginine triad, Arg53, Glu357, and Asp96, is different for both forms of the enzyme, being 3.01 kcal/mol product destabilizing in the apo form and 0.29 kcal/mol product stabilizing in the holo form. As this group of residues represents those that are not as close as the ones mentioned above, this change in the pattern indicates that upon substrate binding the effect exerted on the proton transfer is more localized in the residues that are in direct contact with the substrate.

The change observed in the interaction pattern of the arginine triad upon substrate binding can be qualitatively rationalized by looking at the differences in the charge distribution change seen when the transfer takes place in the apo and holo forms of the enzyme. In Table 2 we show the Mulliken charges (averaged over MD frames) in the product and reactant configuration for TcTS with and without the substrate. The charge of the hydroxyl oxygen of Tyr342 is similar for both systems, when the reactant configuration is considered. After the proton transfer, this oxygen has a larger electron density when the substrate is present than when it is not. This makes the two arginines that are close to Tyr342 (Arg35 and Arg314) stabilize the tyrosinate more in the holo form of TcTS than in its apo form. As has been mentioned Arg245 is H-bonded to the nonacceptor oxygen atom of the carboxylate group of Glu230. This nonacceptor oxygen also possesses a similar charge in the reactant configuration in both systems. In the product state, it has a bigger electron density for the holo form. Although Arg245 destabilizes the reaction, this fact makes it have a smaller destabilizing effect when the substrate is present.

Another fact regarding the charges of the holo form is important to consider in the discussion. In the majority of glycoside hydrolases, a negatively charged nucleophile directly attacks the anomeric C to form the covalent intermediate. Nevertheless, for the case of TcTS, as both the sialic acid and the carboxylate group of Glu230 are negatively charged, this would cause unfavorable interactions. Nature's use of Tyr342 as a nucleophile could be a strategy to avoid a bare negative charge until later in the mechanism. This was stated by Watts et al. (*19*) and can be appreciated in Table 2. For the reactant configuration of the holo form, the total charge of the COH group of Tyr342 (−0.204), although negative, is much smaller than that of the carboxylic group of Glu230 (−1.061). After the transfer of the proton (i.e., product conformation), the tyrosinate nucleophilic attack can take place. In these circumstances the CO^- group of Tyr342 achieves appreciable negative character, with a partial charge of −0.733.

Proton transfer is an essential and ubiquitous step in enzyme catalysis. In most cases the catalyzed reaction starts with the transfer of a proton from the residue to the substrate or the transfer takes place between residues in some step of the mechanism. For this to happen, it is often necessary that the pK_a values of the residues involved are shifted from their solution values. The energy for these changes is stored in the enzyme and prepaid in the folding process (*5*). In the peculiar case presented here, the folding reorganization energy is not enough to make the proton transfer from Tyr342 to Glu230 possible for the apo form of TcTS, but it becomes feasible when the sialyllactose is present in the active site.

CONCLUSIONS

We have carried out QM/MM MD simulations and obtained the free energy profile for the proton transfer that takes place from Tyr342 to Glu230 in the active site of TcTS. The free energy profiles indicate that the transfer is unlikely to happen in the apo form of the enzyme and turns into an energetically possible process only upon substrate binding. By means of the energy decomposition method we calculated the stabilization pattern of the residues of the active site related with the proton transference. This analysis was carried out for the apo and holo forms of TcTS. The global effect in the former case is to destabilize the transference in 3.22 kcal/mol, making the reaction less unlikely than in water solution. When the substrate binds, although it has a destabilizing effect by itself, it causes a change that alters the stabilization pattern that, in this case, is 7.18 kcal/mol product stabilizing. The biggest changes are associated with the arginine triad. These changes in the pattern can be understood in terms of the distinct charge distribution change observed for the transfer in both systems.

ACKNOWLEDGMENT

We thank Johan F. Galindo for his help with graphic support.

REFERENCES

1. Harris, T. K., and Turner, G. (2002) Structural basis of perturbed pK_a values of catalytic groups in enzyme active sites. *IUBMB Life 53*, 85–98.
2. McIntosh, L. P., Hand, G., Johnson, P. E., Joshi, M. D., Korner, M., Plesniak, L. A., Ziser, L., Wakarchuk, W. W., and Withers, S. G. (1991) The pK_a of the general acid/base carboxyl group of a glycosidase cycles during catalysis: a ^{13}C-NMR study of *Bacillus circulans* xylanase. *Biochemistry 35*, 9958–9966.
3. Vocadlo, D. J., Davies, G. J., Laine, R., and Withers, S. G. (2001) Catalysis by hen egg-white lysozyme proceeds via a covalent intermediate. *Nature 412*, 835–838.
4. Nielsen, E. J., and McCammon, A. J. (2003) Calculating pK_a values in enzyme active sites, Vol. 12, Wiley, Malden, MA.
5. Warshel, A., and Papazyan, A. (1996) Energy considerations show that low-barrier hydrogen bonds do not offer a catalytic advantage over ordinary hydrogen bonds. *Proc. Natl. Acad. Sci. U.S.A. 93*, 13665–13670.
6. Warshel, A. (1991) Calculations of enzymic reactions: calculations of pK_a, proton transfer reactions, and general acid catalysis reactions in enzymes. *Biochemistry 20*, 3167–3177.
7. Warshel, A. (1978) Energetics of enzyme catalysis. *Proc. Natl. Acad. Sci. U.S.A. 75*, 5250–5254.
8. Angata, T., and Varki, A. (2002) Chemical diversity in the sialic acids and related α-keto acids: an evolutionary perspective. *Chem. Rev. 102*, 439–470.
9. Schauer, R. (2004) Sialic acids: fascinating sugars in higher animals and man. *Zoology 107*, 49–64.
10. Varki, A. (1997) Sialic acids as ligands in recognition phenomena. *FASEB J. 11*, 248–255.
11. Taylor, G. (1996) Sialidases: structures, biological significance and therapeutic potential. *Curr. Opin. Struct. Biol. 6*, 830–837.
12. Ferrero-Garcia, M. A., Trombetta, S. E., Sanchez, D. O., Reglero, A., Frasch, A. C., and Parodi, A. (1993) The action of *Trypanosoma cruzi* trans-sialidase on glycolipids and glycoproteins. *Eur. J. Biochem. 213*, 765–771.
13. Scudder, P., Doom, J. P., Chuenkova, M., Manger, I. D., and Pereira, M. E. (1993) Enzymatic characterization of beta-D-galactoside alpha 2,3-trans-sialidase from *Trypanosoma cruzi*. *J. Biol. Chem. 268*, 9886–9891.
14. Mucci, J., Hidalgo, A., Mocetti, E., Argibay, P. F., Leguizamón, M. S., and Campetella, O. (2002) Thymocyte depletion in *Trypanosoma cruzi* infection is mediated by trans-sialidase-induced apoptosis on nurse cells complex. *Proc. Natl. Acad. Sci. U.S.A. 99*, 3896–3901.
15. Schenkman, S., Chaves, L. B., Pontes de Carvalho, L. C., and Eichinger, D. (1994) A proteolytic fragment of *Trypanosoma cruzi* trans-sialidase lacking the carboxyl-terminal domain is active, monomeric, and generates antibodies that inhibit enzymatic activity. *J. Biol. Chem. 269*, 7970–7975.
16. Schenkman, S., Jiang, M.-S., Hart, G. W., and Nussenzweig, V. (1991) A novel cell surface trans-sialidase of *Trypanosoma cruzi* generates a stage-specific epitope required for invasion of mammalian cells. *Cell 65*, 1117–1125.
17. Stanley, P. (1984) Glycosylation mutants of animal cells. *Annu. Rev. Genet. 18*, 525–552.
18. Yang, J., Schenkman, S., and Horenstein, B. A. (2000) Primary ^{13}C and β-secondary ^{2}H KIEs for trans-sialidase. A snapshot of nucleophilic participation during catalysis. *Biochemistry 39*, 5902–5910.
19. Watts, A. G., Damager, I., Amaya, M. L., Buschiazzo, A., Alzari, P., Frasch, A. C., and Withers, S. G. (2003) *Trypanosoma cruzi* trans-sialidase operates through a covalent sialyl-enzyme intermediate: tyrosine is the catalytic nucleophile. *J. Am. Chem. Soc. 125*, 7532–7533.
20. Amaya, M., Watts, A. G., Damager, I., Wehenkel, A., Nguyen, T., Buschiazzo, A., Paris, G., Frasch, A. C., Withers, S. G., and Alzari, P. (2004) Structural Insights into the catalytic mechanism of *Trypanosoma cruzi* trans-sialidase. *Structure 12*, 775–784.
21. Demir, O. z., and Roitberg, A. (2009) Modulation of catalytic function by differential plasticity of the active site: case study of *Trypanosoma cruzi* trans-sialidase and *Trypanosoma rangeli* sialidase. *Biochemistry 48*, 3398–3406.
22. Horenstein, B., and Y. J., Bruner, M. (2002) Mechanistic variation in the glycosyltransfer of N-acetylneuraminic acid. *Nukleonika 47* (Suppl. 1), S25–S28.
23. Kirby, A. J. (1987) Mechanism and stereoelectronic effects in the lysozyme reaction. *Crit. Rev. Biochem. Mol. Biol. 22*, 283–315.
24. Phillips, D. C. (1967) The hen egg-white lysozyme molecule. *Proc. Natl. Acad. Sci. U.S.A. 57*, 483–495.
25. Frisch, M. J., Trucks, G. W., Schlegel, H. B., Scuseria, G. E., Robb, M. A., Cheeseman, J. R., Scalmani, G., Barone, V., Mennucci, B., Petersson, G. A., Nakatsuji, H., Caricato, M., Li, X., Hratchian, H. P., Izmaylov, A. F., Bloino, J., Zheng, G., Sonnenberg, J. L., Hada, M., Ehara, M., Toyota, K., Fukuda, R., Hasegawa, J., Ishida, M., Nakajima, T., Honda, Y., Kitao, O., Nakai, H., Vreven, T., Montgomery, Jr., J. A., Peralta, J. E., Ogliaro, F., Bearpark, M., Heyd, J. J., Brothers, E., Kudin, K. N., Staroverov, V. N., Kobayashi, R., Normand, J., Raghavachari, K., Rendell, A., Burant, J. C., Iyengar, S. S., Tomasi, J., Cossi, M., Rega, N., Millam, N. J., Klene, M., Knox, J. E., Cross, J. B., Bakken, V., Adamo, C., Jaramillo, J., Gomperts, R., Stratmann, R. E., Yazyev, O., Austin, A. J., Cammi, R., Pomelli, C., Ochterski, J. W., Martin, R. L., Morokuma, K., Zakrzewski, V. G., Voth, G. A., Salvador, P., Dannenberg, J. J., Dapprich, S., Daniels, A. D., Farkas, Ö., Foresman, J. B., Ortiz, J. V., Cioslowski, J., and Fox, D. J. (2009) Gaussian 09, Revision A.02, Gaussian, Inc., Wallingford, CT.
26. Case, D. A., Darden, T. A., Cheatham, T. E., III, Simmerling, C. L., Wang, J., Duke, R. E., Luo, R., Crowley, M., W., R. C., Zhang, W., Merz, K. M., Wang, B., Hayik, S., Roitberg, A., Seabra, G., Kolossváry, I., Wong, K. F., Paesani, F., Vanicek, J., Wu, X., Brozell, S. R., Steinbrecher, T., Gohlke, H., Yang, L., T., C., Mongan, J., Hornak, V., Cui, G., Mathews, D. H., Seetin, M. G., Sagui, C., Babin, V., and Kollman, A. P. A. (2008) University of California, San Francisco.
27. Repasky, M. P., Chandrasekhar, J., and Jorgensen, W. (2002) PDDG/PM3 and PDDG/MNDO: improved semiempirical methods. *J. Comput. Chem. 23*, 1601–1622.
28. Hornak, V., Abel, R., Okur, A., Strockbine, B., Roitberg, A., and Simmerling, C. (2006) Comparison of multiple Amber force fields and development of improved protein backbone parameters. *Proteins: Struct., Funct., Bioinf. 65*, 712–725.
29. Cornell, W. D., Cieplak, P., Bayly, C. I., Gould, I. R., Merz, K. M., Ferguson, D. M., Spellmeyer, D. C., Fox, T., Caldwell, J. W., and

Kollman, P. (1995) A second generation force field for the simulation of proteins, nucleic acids, and organic molecules. *J. Am. Chem. Soc. 117*, 5179–5197.
30. Darden, T., York, D., and Pedersen, L. (1993) Particle mesh Ewald: an N·log(N) method for Ewald sums in large systems. *J. Chem. Phys. 98*, 10089–10092.
31. Berendsen, H. J. C., Postma, J. P. M., van Gunsteren, W. F., Dinola, A., and Haak, J. R. (1984) Molecular dynamics with coupling to an external bath. *J. Chem. Phys. 81*, 3684–3690.
32. Kumar, S., Rosenberg, J. M., Bouzida, D., Swendsen, R. H., and Kollman, P. (1992) The weighted histogram analysis method for free-energy calculations on biomolecules. I: The method. *J. Comput. Chem. 13*, 1011–1021.
33. Lin, Y., and Gao, J. (2010) Internal proton transfer in the external pyridoxal 5′-phosphate Schiff base in Dopa decarboxylase. *Biochemistry 49*, 84–94.
34. Chatfield, D. C., P. Eurenius, K., and Brooks, B. R. (1998) HIV-1 protease cleavage mechanism: a theoretical investigation based on classical MD simulation and reaction path calculations using a hybrid QM/MM potential. *J. Mol. Struct.: THEOCHEM 423*, 79–92.
35. Cunningham, M. A., Ho, L. L., Nguyen, D. T., Gillilan, R. E., and Bash, P. A. (1997) Simulation of the enzyme reaction mechanism of malate dehydrogenase. *Biochemistry 36*, 4800–4816.
36. Davenport, R. C., Bash, P. A., Seaton, B. A., Karplus, M., Petsko, G. A., and Ringe, D. (1991) Structure of the triosephosphate isomerase-phosphoglycolohydroxamate complex: an analog of the intermediate on the reaction pathway. *Biochemistry 30*, 5821–5826.
37. Dinner, A. R., Blackburn, G. M., and Karplus, M. (2001) Uracil-DNA glycosylase acts by substrate autocatalysis. *Nature 413*, 752–755.
38. Garcia-Viloca, M., Truhlar, G. D., and Gao, J. (2003) Reaction-path energetics and kinetics of the hydride transfer reaction catalyzed by dihydrofolate reductase. *Biochemistry 42*, 13558–13575.
39. Hensen, C., Hermann, C. J., Nam, K., Ma, S., Gao, J., and Höltje, H. (2004) A combined QM/MM approach to protein-ligand interactions: polarization effects of the HIV-1 protease on selected high affinity inhibitors. *J. Med. Chem. 47*, 6673–6680.
40. Major, D. T., and Gao, J. (2006) A combined quantum mechanical and molecular mechanical study of the reaction mechanism and α-amino acidity in alanine racemase. *J. Am. Chem. Soc. 128*, 16345–16357.
41. Wong, K., and Gao, J. (2007) The reaction mechanism of paraoxon hydrolysis by phosphotriesterase from combined QM/MM simulations. *Biochemistry 46*, 13352–13369.
42. Gao, J., and Xia, X. (1992) A priori evaluation of aqueous polarization effects through Monte Carlo QM-MM simulations. *Science 258*, 631–635.
43. Garcia-Viloca, M., Truhlar, D. G., and Gao, J. (2003) Importance of substrate and cofactor polarization in the active site of dihydrofolate reductase. *J. Mol. Biol. 327*, 549–560.
44. Orozco, M., Luque, F. J., Habibollahzadeh, D., and Gao, J. (1995) The polarization contribution to the free energy of hydration. *J. Chem. Phys. 102*, 6145–6152.
45. Gao, J. (1996) Hybrid quantum and molecular mechanical simulations: an alternative avenue to solvent effects in organic chemistry. *Acc. Chem. Res. 29*, 298–305.
46. Gao, J. (1995) An automated procedure for simulating chemical reactions in solution. Application to the decarboxylation of 3-carboxybenzisoxazole in water. *J. Am. Chem. Soc. 117*, 8600–8607.
47. Mo, Y., and Gao, J. (2000) *Ab initio* QM/MM simulations with a molecular orbital-valence bond (MOVB) method: application to an S_N2 reaction in water. *J. Comput. Chem. 21*, 1458–1469.
48. Acevedo, O., and Jorgensen, W. (2009) Advances in quantum and molecular mechanical (QM/MM) simulations for organic and enzymatic reactions. *Acc. Chem. Res. 43*, 142–151.
49. Zhou, M. M., Davis, J. P., and Van Etten, R. L. (1993) Identification and pK_a determination of the histidine residues of human low-molecular-weight phosphotyrosyl protein phosphatases: a convenient approach using MLEV-17 spectral editing scheme. *Biochemistry 32*, 8479–8486.
50. Lamotte-Brasseur, J., Dubus, A., and Wade, R. C. (2000) pK_a calculations for class C β-lactamases: the role of Tyr-150. *Proteins: Struct., Funct., Bioinf. 40*, 23–28.
51. Chivers, P. T., Prehoda, K. E., Volkman, B. F., Kim, B., Markley, J. L., and Raines, R. T. (1997) Microscopic pK_a values of *Escherichia coli* thioredoxin. *Biochemistry 36*, 14985–14991.